CONF-840275--10

EFI 84/8

FORWARD-BACKWARD ASYMMETRIES IN W AND Z DECAYS*

CONF-840275--10

DE84 013481

Jonathan L. Rosner
Enrico Fermi Institute and Department of Physics
University of Chicago, Chicago, IL 60637

Paul Langacker
Department of Physics
University of Pennsylvania, Philadelphia, PA 19104, and
Institute for Advanced Study, and Princeton, NJ 08540

Richard W. Robinett
Department of Physics
University of Massachusetts, Amherst, MA 01003

ABSTRACT

The leptons emitted in decays of W and Z bosons produced in pp or $\bar{p}p$ collisions exhibit characteristic asymmetries with respect to the beam direction, as measured in the W or Z center-of-mass. The asymmetries appear in both pp and $\bar{p}p$ collisions. For $\bar{p}p$ collisions they appear to be approximately constant over the whole y range for values of $M/\sqrt{s} \gtrsim 0.1$ For smaller values of $M/\sqrt{s}$, the asymmetries become more and more washed out in the central region as sea-sea collisions begin to play a larger role in gauge boson formation.

INTRODUCTION

Forward-backward asymmetries in W decays have played a crucial role in establishing that the spin of the W is 1.[1] They can also be expected to be useful in identifying the characteristic couplings of the Z° and of any other new, heavy gauge bosons that could be produced. Such possible gauge bosons include:

(1) a massive counterpart W_R of the W,[2] coupled via right-handed currents to ordinary matter; and

(2) heavier Z's, which arise when one gauges more U(1) symmetries than simply the weak hypercharge.[3]

TABLE 1. Gauge bosons examined for decay asymmetries of the underlined leptons. Here N is a right-handed neutrino, which may be massive.

Boson	Mass	Decay	Comments
W	81 GeV	$\underline{\ell}\nu$	Standard left-handed W
Z	92 GeV	$\underline{\ell}^-\ell^+$	Standard model Z
W_R	2 TeV	$\underline{\ell}N$	Right-handed W
Z_X	1 TeV	$\underline{\ell}^-\ell^+$	Couplings defined in Appendix

MASTER

*Presented by J. Rosner at DPF Workshop on $\bar{p}p$ Options for the Super Collider, University of Chicago, Feb. 13-17, 1984.

In this note we display some of the expected forward-backward asymmetries for various possibilities, listed in Table 1.

We first discuss production of the bosons in Table 1, then their decay asymmetries. Some experimental possibilities for observing these asymmetries have been studied separately. A longer version of this note, dealing with this and other aspects of heavy gauge boson production in pp and $\bar{p}p$ collisions, is anticipated.[5]

PRODUCTION CROSS SECTIONS AND RAPIDITY DISTRIBUTIONS

We assume that W's and Z's are produced with zero transverse momenta via standard couplings to quarks and antiquarks. For the Z_x the assumptions leading to couplings are described in the Appendix. The resulting y distributions are obtained using structure functions of Ref. 6. We then find

$$B\frac{d\sigma}{dy}(AB \to W^{\pm}+..)_{\hookrightarrow \ell^{\pm}\nu} = \frac{8.87\times10^{-3}}{s}\left\{\begin{array}{c} U_A\bar{D}_B+\bar{D}_AU_B \\ D_A\bar{U}_B+\bar{U}_AD_B \end{array}\right\} \tag{1}$$

$$B\frac{d\sigma}{dy}(AB \to Z^{\circ}_{\hookrightarrow \ell^-\ell^+}) = \frac{1.31\times10^{-3}}{s}(U_A\bar{U}_B+\bar{U}_AU_B) + \frac{1.67\times10^{-3}}{s}(D_A\bar{D}_B+\bar{D}_AD_B) \tag{2}$$

$$B\frac{d\sigma}{dy}(AB \to Z_{x\,\hookrightarrow \ell^-\ell^+}) = \frac{2.22\times10^{-4}}{s}(U_A\bar{U}_B+\bar{U}_AU_B) + \frac{1.11\times10^{-3}}{s}(D_A\bar{D}_B+\bar{D}_AD_B). \tag{3}$$

The numerical coefficients in (1)-(3) are dimensionless. Here we have used an 8.3% branching ratio for $W^{\pm} \to \ell^{\pm}\nu$ (or $\ell^{\pm}N$ for W_R), 3.1% for $Z^{\circ} \to \ell^-\ell^+$ and 4.16% (=1/24) for $Z_x \to \ell^-\ell^+$. This last number is explained in the Appendix. Eqs. (1)-(3) are valid for any mass of W or Z. Here, for example,

$$U_A\bar{D}_B = U_A(x_1)\bar{D}_B(x_2), \tag{4}$$

with $$x_1x_2 = M^2/s \tag{5}$$

and $$\left.\begin{array}{c} x_1 \\ x_2 \end{array}\right\} = \frac{M}{\sqrt{s}}e^{\pm y} \tag{6}$$

We show the resulting values of $B\frac{d\sigma}{dy}$ for $W^{\pm}$ and $W_R^{\pm}$ in Figs. 1 and 2. The rapidity y shown is that of the gauge boson. The rapidity y_ℓ of the observed lepton is related to y by $\tanh(y_\ell - y) = \cos\theta^*$, where θ^* is the angle of the lepton in the gauge boson center-of-mass relative to the direction defined by $y>0$. Since, as shown below, the gauge boson decay distribution is a low-order polynomial in $\cos\theta^*$, most of the leptons will be emitted with rapidities within 1 or 2 units of y, independent of the gauge boson or lepton mass. (There will be a tiny tail of very high-rapidity leptons, whose length does depend on these masses).

In plotting Figs. 1 and 2 we have assumed that both leptons have a maximum observable $|y_\ell|$ arbitrarily taken as 6 in Fig. 1 and 4 in Fig. 2. (For ordinary W decays we assume that the missing neutrino is not observable beyond a certain rapidity, because its transverse momentum is too low. For convenience we take this to be equal to the maximum observable charged lepton rapidity.)

The effects of valence quarks can be clearly seen by a comparison of pp and $p\bar{p}$ production of W^+ at very high energies (10-40 TeV). The y distributions in pp $\to W^+$ have two "wings"; those in $p\bar{p}$ have only one. It is thus apparent that valence quarks can play a crucial role in gauge boson production away from y=0 even at very high energies.

FORWARD-BACKWARD ASYMMETRIES

The role of valence quarks is very striking in the determination of forward-backward asymmetries. These may be calculated by noting that, in the quark-antiquark center-of-mass,

$$\frac{d\sigma}{d\Omega}(q_1\bar{q}_2 \to \text{gauge boson} \to \ell_1\bar{\ell}_2)$$
$$\sim (L_{q_1}^2 L_{\ell_1}^2 + R_{q_1}^2 R_{\ell_1}^2)(1+\cos\theta^*)^2$$
$$+ (L_{q_1}^2 R_{\ell_1}^2 + R_{q_1}^2 L_{\ell_1}^2)(1-\cos\theta^*)^2. \qquad (7)$$

Here L_q, R_q, L_ℓ, R_ℓ denote left-handed and right-handed couplings of quarks and leptons. The differential cross-sections per unit of rapidity and per unit of lepton solid angle in the gauge boson c.m.s. are thus:

W^+ production: (ℓ^+ angle)

$$\frac{d^2\sigma}{dy\,d\Omega} \sim U(x_1)\bar{D}(x_2)(1-\cos\theta^*)^2$$
$$+ \bar{D}(x_1)U(x_2)(1+\cos\theta^*)^2 \qquad (8)$$

W^- production: (ℓ^- angle)

$$\frac{d^2\sigma}{dy\,d\Omega} \sim D(x_1)\bar{U}(x_2)(1+\cos\theta^*)^2$$
$$+ \bar{U}(x_1)D(x_2)(1-\cos\theta^*)^2 \qquad (9)$$

Z production: (ℓ^- angle)

$$\frac{d^2\sigma}{dy\,d\Omega} \sim [(L_u^2L_\ell^2 + R_u^2R_\ell^2)(U(x_1)\bar{U}(x_2))$$

$$+(L_u^2R_\ell^2 + R_u^2L_\ell^2)(\bar{U}(x_1)U(x_2))](1+\cos\theta^*)^2$$

$$+ [(L_u^2L_\ell^2 + R_u^2R_\ell^2)(\bar{U}(x_1)U(x_2))$$

$$+(L_u^2R_\ell^2 + R_u^2L_\ell^2)(U(x_1)\bar{U}(x_2))]\ (1-\cos\theta^*)^2$$

$$+ (U \to D) \quad . \qquad (10)$$

The relative squares of left-handed and right-handed couplings to Z_0 and Z_χ are shown in Table 2.

TABLE 2. Relative squares of left-handed and right-handed couplings of fermion-antifermion pairs to Z_0 and Z_χ.

Coupling	Z_0	Z_χ
L_ℓ^2	$(-1+2x)^2 = 0.314$	9
R_ℓ^2	$(2x)^2 = 0.194$	1
L_u^2	$(1 - \frac{4}{3}x)^2 = 0.499$	1
R_u^2	$(-\frac{4}{3}x)^2 = 0.086$	1
L_d^2	$(-1 + \frac{2}{3}x)^2 = 0.728$	1
R_d^2	$(\frac{2}{3}x)^2 = 0.022$	9

The corresponding values of

$$\left.\frac{d\sigma}{dy}\right|_{F\pm B} \sim \left(\int_0^1 \pm \int_{-1}^0\right) d(\cos\theta)\ \frac{d^2\sigma}{dy\,d\Omega} \qquad (11)$$

are

$$\left.\frac{d\sigma}{dy}\right|_{F\pm B}(W^+ \to \ell^+) \sim \pm U(x_1)\bar{D}(x_2)+\bar{D}(x_1)U(x_2) \qquad (12)$$

$$\left.\frac{d\sigma}{dy}\right|_{F\pm B}(W^- \to \ell^-) \sim D(x_1)\bar{U}(x_2) \pm \bar{U}(x_1)D(x_2) \tag{13}$$

$$\left.\frac{d\sigma}{dy}\right|_{F\pm B}(Z \to \ell^-) \sim [(U(x_1)\bar{U}(x_2) \pm \bar{U}(x_1)U(x_2)) \times (L_u^2 \pm R_u^2)][L_\ell^2 \pm R_\ell^2] + (U \to D) \quad , \tag{14}$$

$$A_{FB} \equiv \frac{(d\sigma/dy)_F - (d\sigma/dy)_B}{(d\sigma/dy)_F + (d\sigma/dy)_B} \quad .. \tag{15}$$

At fixed y one then can plot forward-backward asymmetries. The results are shown in Figs. 3-8. Several comments are in order.

(1) Asymmetries in proton-proton collisions do not vanish, except at y=0. They are odd in y, rising (or falling) to very near the maximum (or minimum) values attained in $p\bar{p}$ collisions at the same energy when one moves away from y=0.

(2) For $M/\sqrt{s} \gtrsim 0.1$, asymmetries in $p\bar{p}$ collisions are nearly constant over a wide y range. As $\sqrt{s}$ increases, these asymmetries become washed out in the central region as sea-sea collisions begin to play a larger role in gauge boson formation.

(3) The asymmetries in Z production are very sensitive to the specific forms of couplings.

The practical observation of asymmetries in pp collisions requires the binning of data with respect to rapidity. This will lead to a loss of data around y=0, but still should yield useful results. The question is being examined in more detail for a specific detector design.[3] It may also be possible to construct more global variables (such as average lepton energy) sensitive to these asymmetries.[5]

ACKNOWLEDGEMENTS

We are grateful to the authors of Ref. 6 for discussions and for providing us with numerical values of their structure functions. We thank P. Darriulat, M. K. Gaillard, G. Gollin, F. Paige, and E. Witten for helpful conversations. This work was supported in part by the U. S. Department of Energy under contracts No. DE-AC02-82ER40073 (Chicago) and EY76C-02-3071 (Pennsylvania), by the National Science Foundation under Contract No. PHY-83014062 (University of Massachusetts), and by the Institute for Advanced Study.

APPENDIX. Couplings of Z_χ.

The normal expression for the charge in the standard model is

$$Q = I_{3L} + \frac{Y}{2} \qquad (A.1)$$

Both I_{3L} and Y are gauged. If one extends the model to one in which the possibility of left-right symmetry at higher energies is entertained, one can write

$$\frac{Y}{2} = I_{3R} + \frac{B-L}{2} \qquad (A.2)$$

and gauge both I_{3R} and $\frac{B-L}{2}$. The demand that I_{3R} and $\frac{B-L}{2}$ be anomaly-free with respect to members of a multiplet then can be met if one introduces a right-handed neutrino N, which may have a large Majorana mass. It is then possible to normalize I_{3L}, I_{3R}, and $(B-L)/2$ consistently over members of a generation of quarks and leptons

$$\Sigma\, I_{3L}^2 = \Sigma\, I_{3R}^2 = \Sigma\, N^2\left(\frac{B-L}{2}\right)^2 \qquad (A.3)$$

where $N\,\frac{B-L}{2}$ is a generator proportional to $(B-L)/2$ with the same normalization as I_{3L} and I_{3R}. There is then a combination of I_{3R} and $N\,\frac{B-L}{2}$ orthogonal to that shown in (A.2). It is proportional to

$$\chi \equiv 2I_{3R} - \frac{3}{2}\left(\frac{B-L}{2}\right) = 5I_{3R} + 3(I_{3L} - Q). \qquad (A.4)$$

The values of χ for various left-handed quarks and leptons are shown in Table A.1. These are just the values of the U(1) charge in $SO(10) \rightarrow SU(5) \times U(1)$, but of course are more general. The charge χ is likely to be of interest whenever one attempts to gauge both I_{3R} and $(B-L)/2$.

TABLE A.1. Values of generator χ for left-handed fermions.

$\chi = 3$:	d, e^-, ν	SU(5) 5-plet
$\chi = -1$:	$u, \bar{u}, \bar{d}, e^+$	SU(5) 10*-plet
$\chi = -5$:	$\bar{N}$	SU(5) singlet
		SO(10) 16*-plet

$\Gamma(Z_\chi \rightarrow u\bar{u} : d\bar{d} : e^+e^- : \nu_e\bar{\nu}_e : N_e\bar{N}_e) =$

$= 3(1^2+1^2) : 3(3^2+1^2) : 3^2+1^2 : 3^2 : 5^2 = 6 : 30 : 10 : 9 : 25$

For 3 generations, $B(Z_\chi \rightarrow e^+e^-) = (1/3)\,(10/80) = 1/24$.

FIGURES

Fig. 1. $B_{e\nu}(d\sigma/dy)$ for pp, $p\bar{p} \rightarrow W^{\pm}$ at E_{CM} = 40 TeV. Solid line: $p\bar{p} \rightarrow W^{+}$ (p along +y direction here and elsewhere). For $p\bar{p} \rightarrow W^{-}$, reflect this curve about y=0. Dashed line: $pp \rightarrow W^{+}$. Dotted line: $pp \rightarrow W^{-}$.

Fig. 2. $B_{eN}(d\sigma/dy)$ for pp, $p\bar{p} \rightarrow W_R^{\pm}$ at E_{CM} = 40 TeV. Solid, dashed, and dotted lines as in Fig. 1. (Here we show both charges of W_R in $p\bar{p}$ interactions).

Fig. 3. Forward-backward asymmetries A_{FB} of ℓ^{+} in W^{+} c.m.s. as functions of W^{+} rapidity y_{W^+} in pp (dashed-lines) and $p\bar{p}$ (solid lines) $\rightarrow W^{+} \rightarrow \ell^{+}\nu$. Curves are labeled by total c.m. energy in TeV.

Fig. 4. Same as Fig. 3 for W^{-}, ℓ^{-}.

Fig. 5. A_{FB} of ℓ^{-} vs. y_{Z° in pp (dashed lines and $p\bar{p}$ (solid lines) $\rightarrow Z^{\circ} \rightarrow \ell^{-}\ell^{+}$.

Fig. 6. A_{FB} of ℓ^{+} in W_R^{+} c.m.s. for M_{W_R} = 2 TeV, vs. $y_{W_R}{}^{+}$. (Other labels as in Fig. 3).

Fig. 7. Same as Fig. 6 for W_R^{-}, ℓ^{-}.

Fig. 8. A_{FB} of ℓ^{-} vs. y_{Z_X} for M_Z = 1 TeV, vs. y_{Z_X}. (Other labels as in Fig. 5).

REFERENCES

† Permanent address.

1. C. Rubbia, this conference.
2. J. C. Pati and A. Salam, Phys. Rev. Lett. 31, 661 (1973); Phys. Rev. D10, 275 (1974); R. N. Mohapatra and J. C. Pati, ibid, 11, 566, 2558 (1975).
3. See Ref. 2 as well as N. Deshpande and D. Iskandar, Phys. Rev. Lett. 42, 20 (1979); Phys. Lett. 87B, 383 (1979); Nucl. Phys. B107, 223 (1980); R. W. Robinett and J. L. Rosner, Phys. Rev. D25, 3036 (1982); C. N. Leung and J. L. Rosner, FERMILAB-Pub-83/90-THY/Rev., to be published in Phys. Rev. D.
4. G. Gollin, this conference.
5. P. Langacker, R.W. Robinett, and J.L. Rosner, in preparation.
6. E. Eichten, I. Hinchliffe, K. Lane, and C. Quigg, FERMILAB-Pub-84/17-THY, to be published in Rev. Mod. Phys.

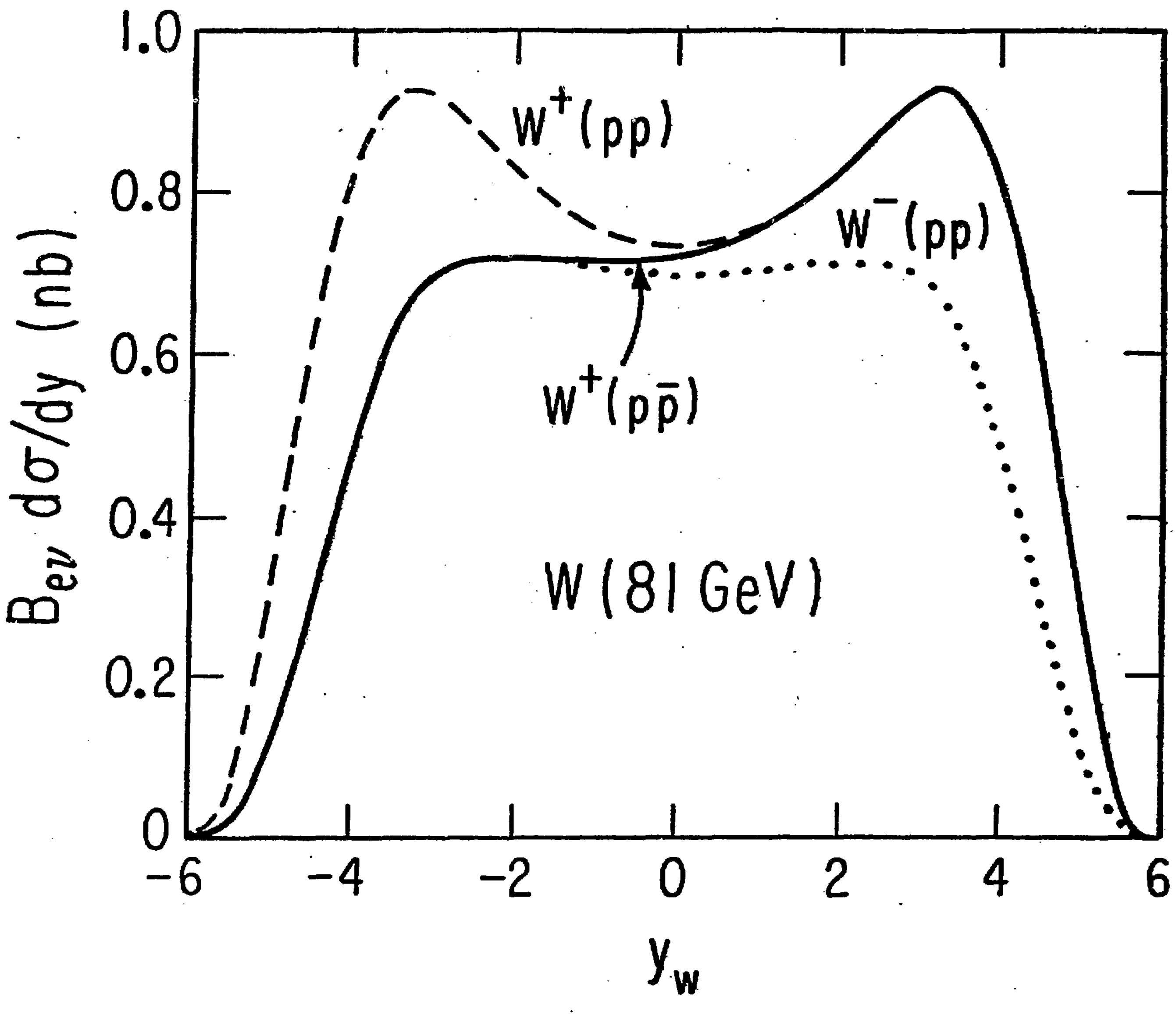

1.0
0.8
0.6
0.4
0.2
0
$B_{e\nu}\ d\sigma/dy$ (nb)
$W^+(pp)$
$W^-(pp)$
$W^+(p\bar{p})$
W (81 GeV)
-6
-4
-2
0
2
4
6
y_W

FIGURE 1

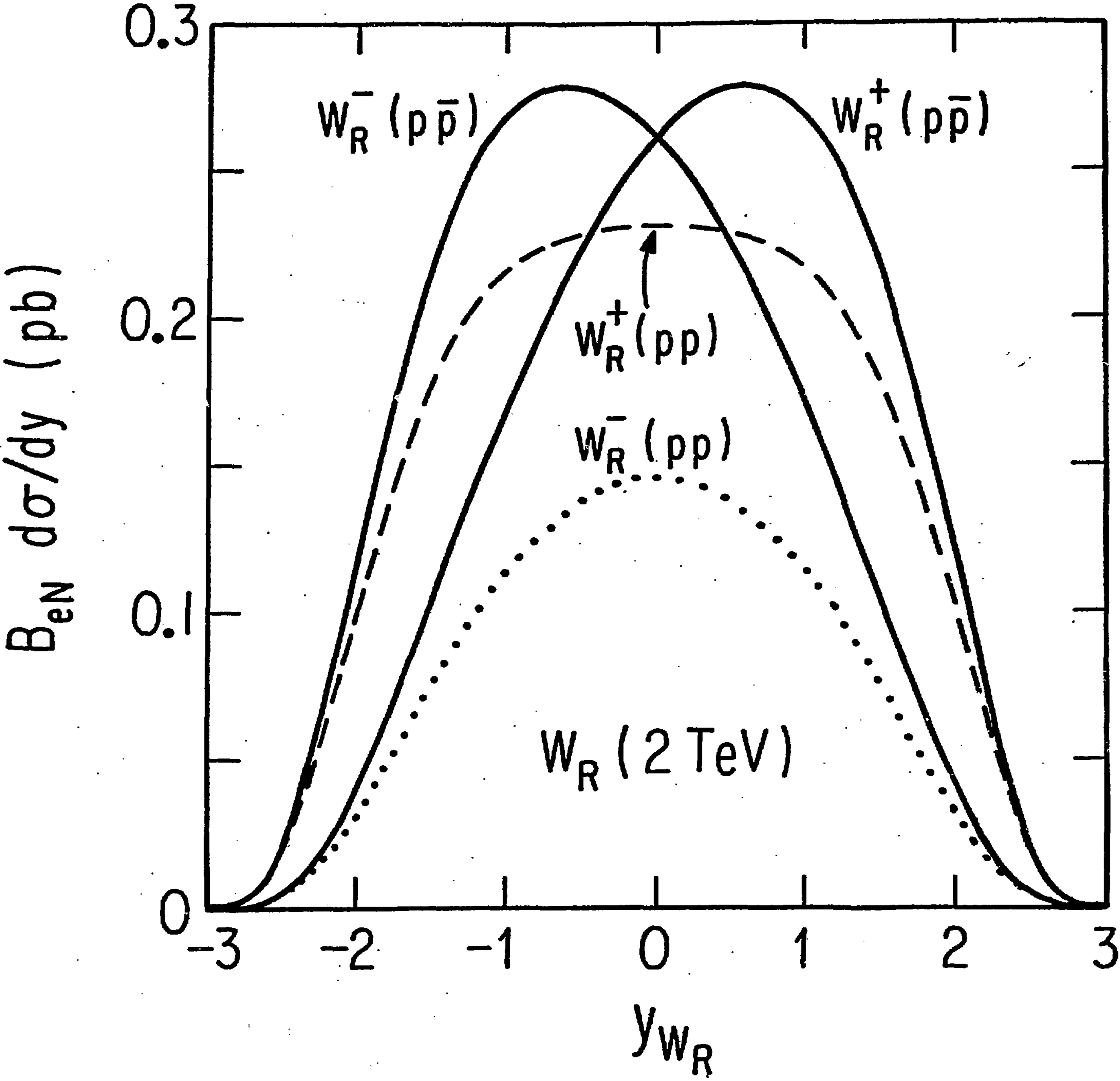
0.3
0.2
0.1
0
$B_{eN}\ d\sigma/dy$ (pb)
$W_R^-\ (p\bar{p})$
$W_R^+\ (p\bar{p})$
$W_R^+\ (pp)$
$W_R^-\ (pp)$
W_R (2 TeV)
−3
−2
−1
0
1
2
3
y_{W_R}

FIGURE 2

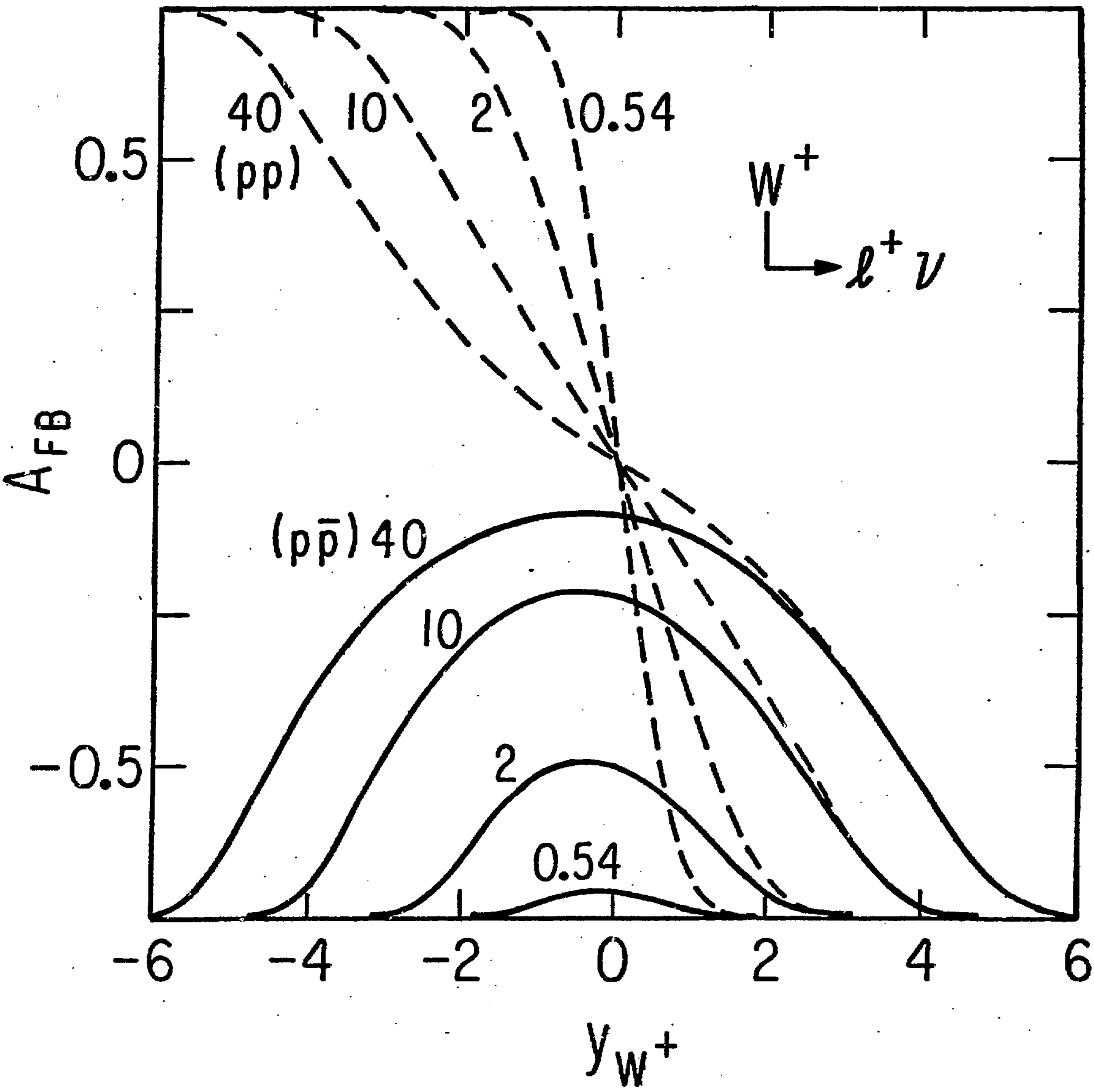

FIGURE 3

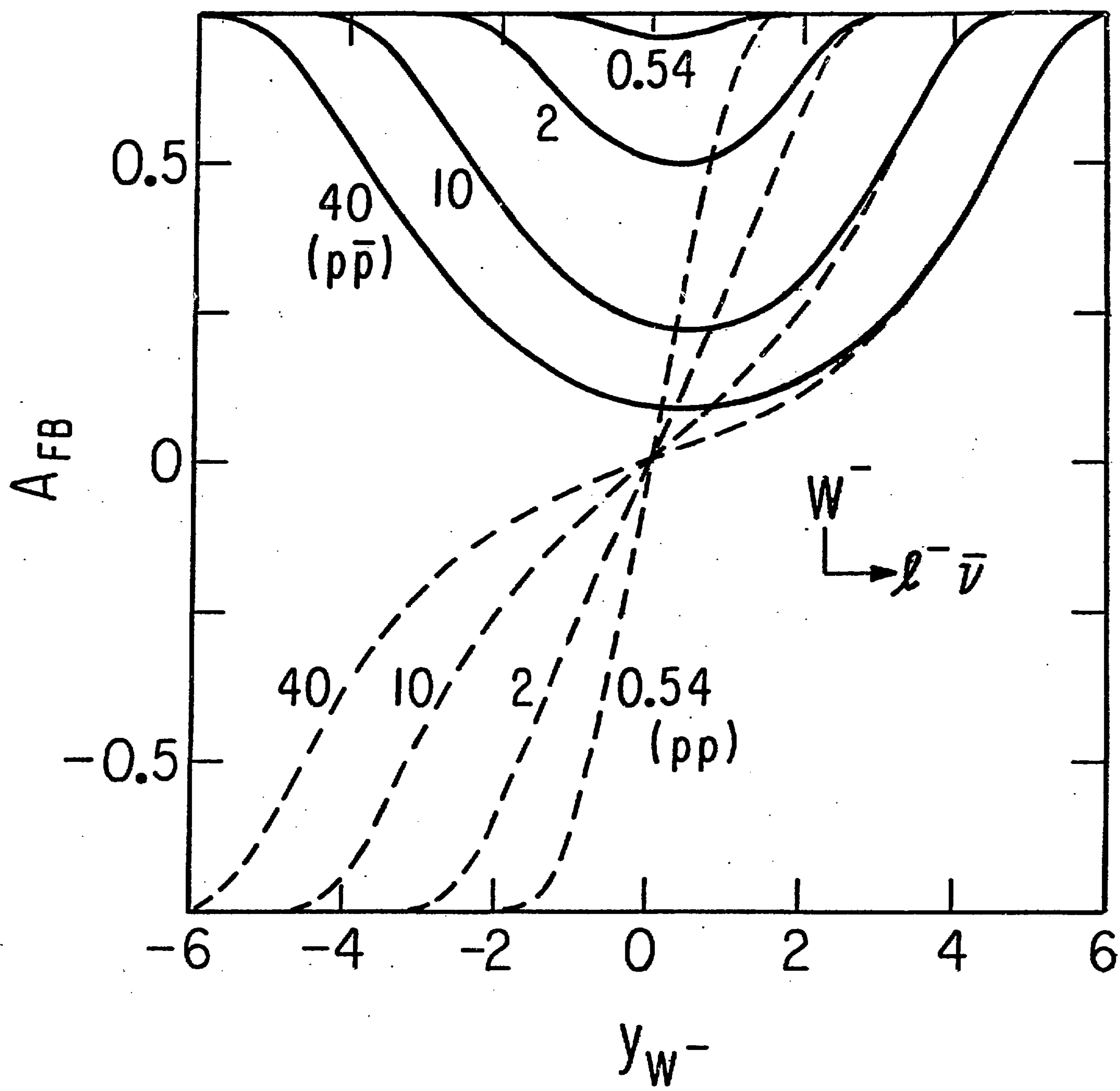

FIGURE 4

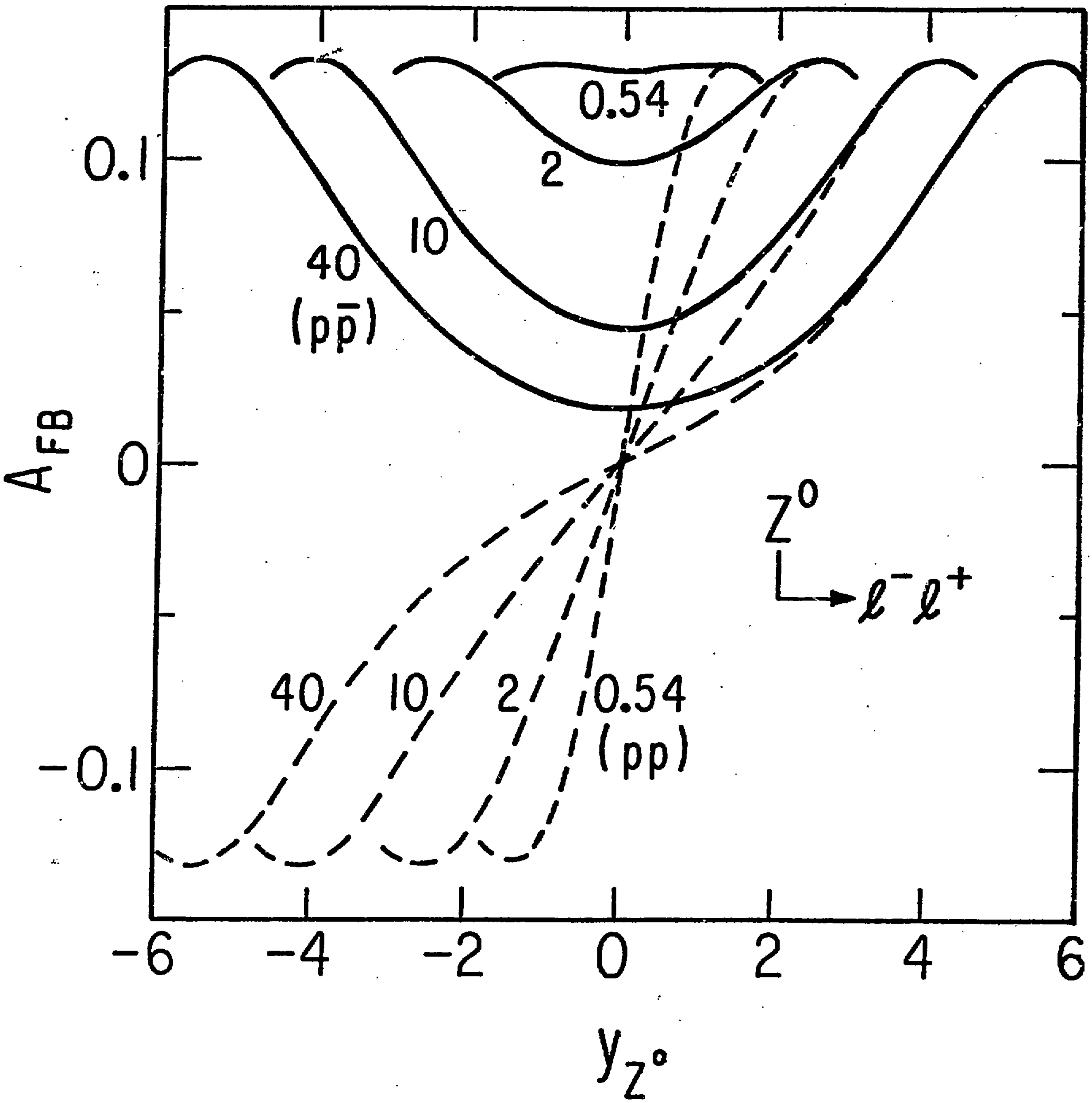

0.1
0
−0.1
A_{FB}
0.54
2
10
40
(p$\bar{p}$)
Z^0
$\ell^-\ell^+$
40
10
2
0.54
(pp)
−6
−4
−2
0
2
4
6
y_{Z°

FIGURE 5

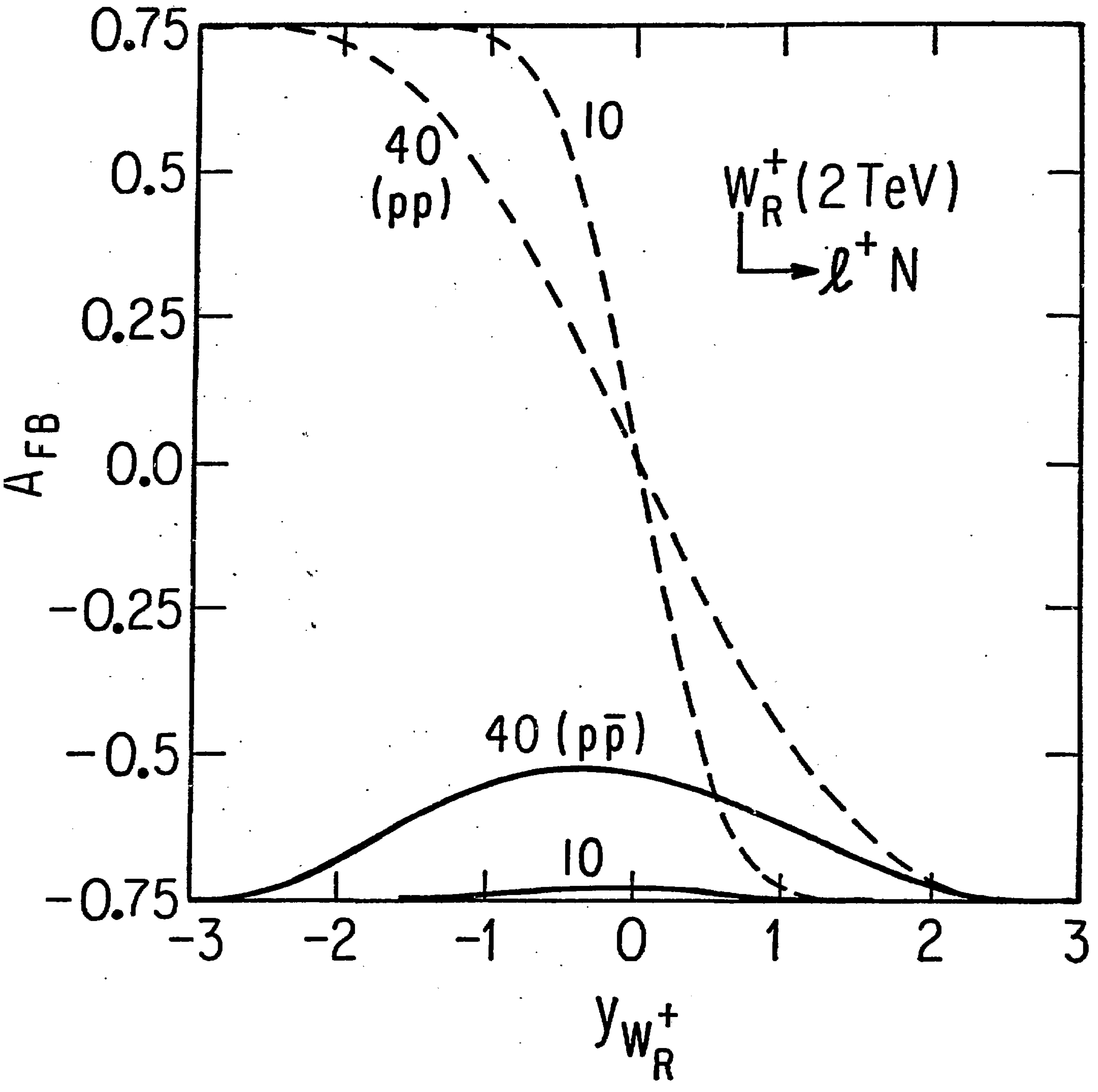
0.75
0.5
0.25
0.0
−0.25
−0.5
−0.75
A_{FB}
10
40
(pp)
W_R^+(2 TeV)
$\ell^+ N$
40 ($p\bar{p}$)
10
−3
−2
−1
0
1
2
3
$y_{W_R^+}$

FIGURE 6

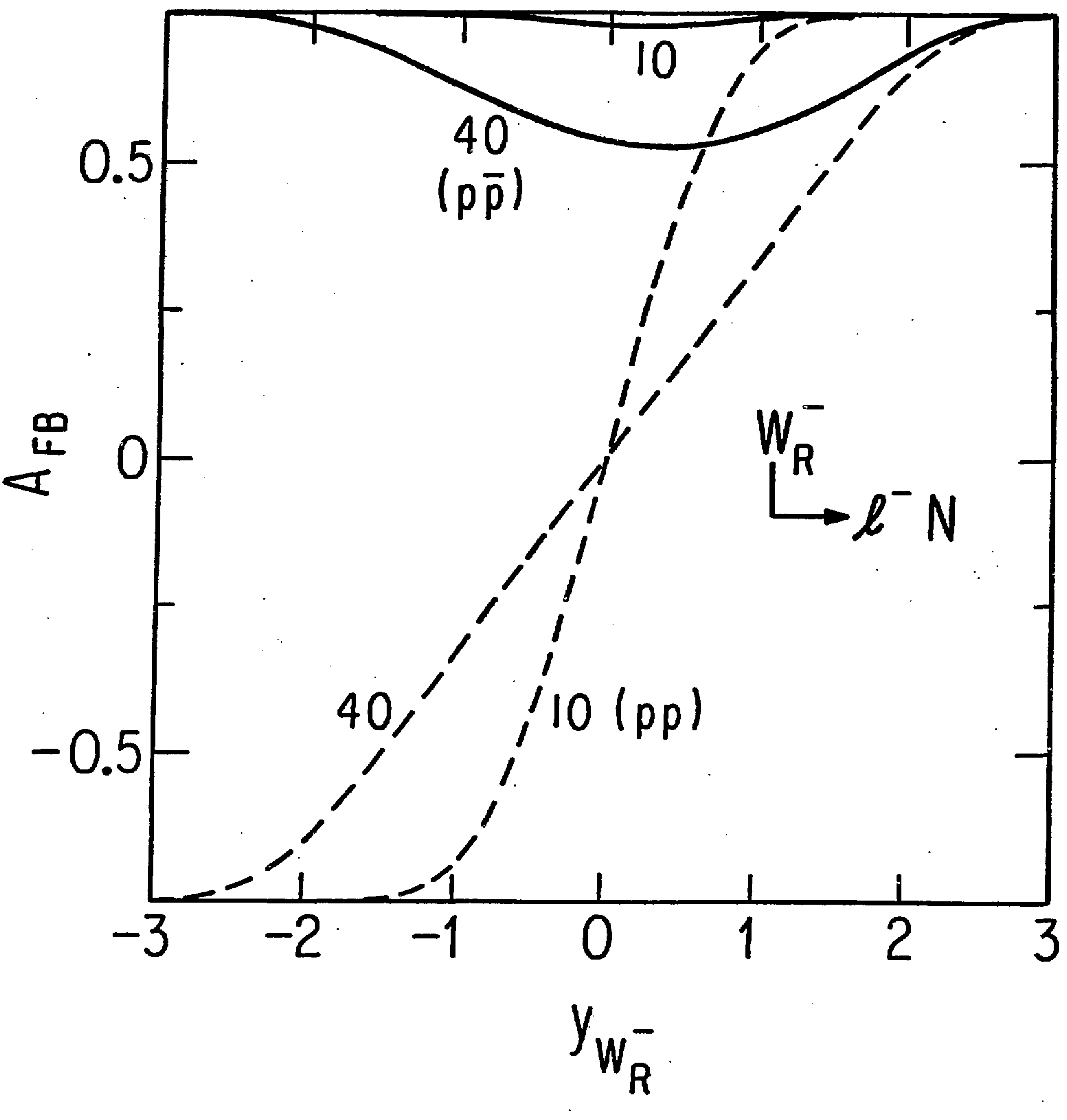

FIGURE 7

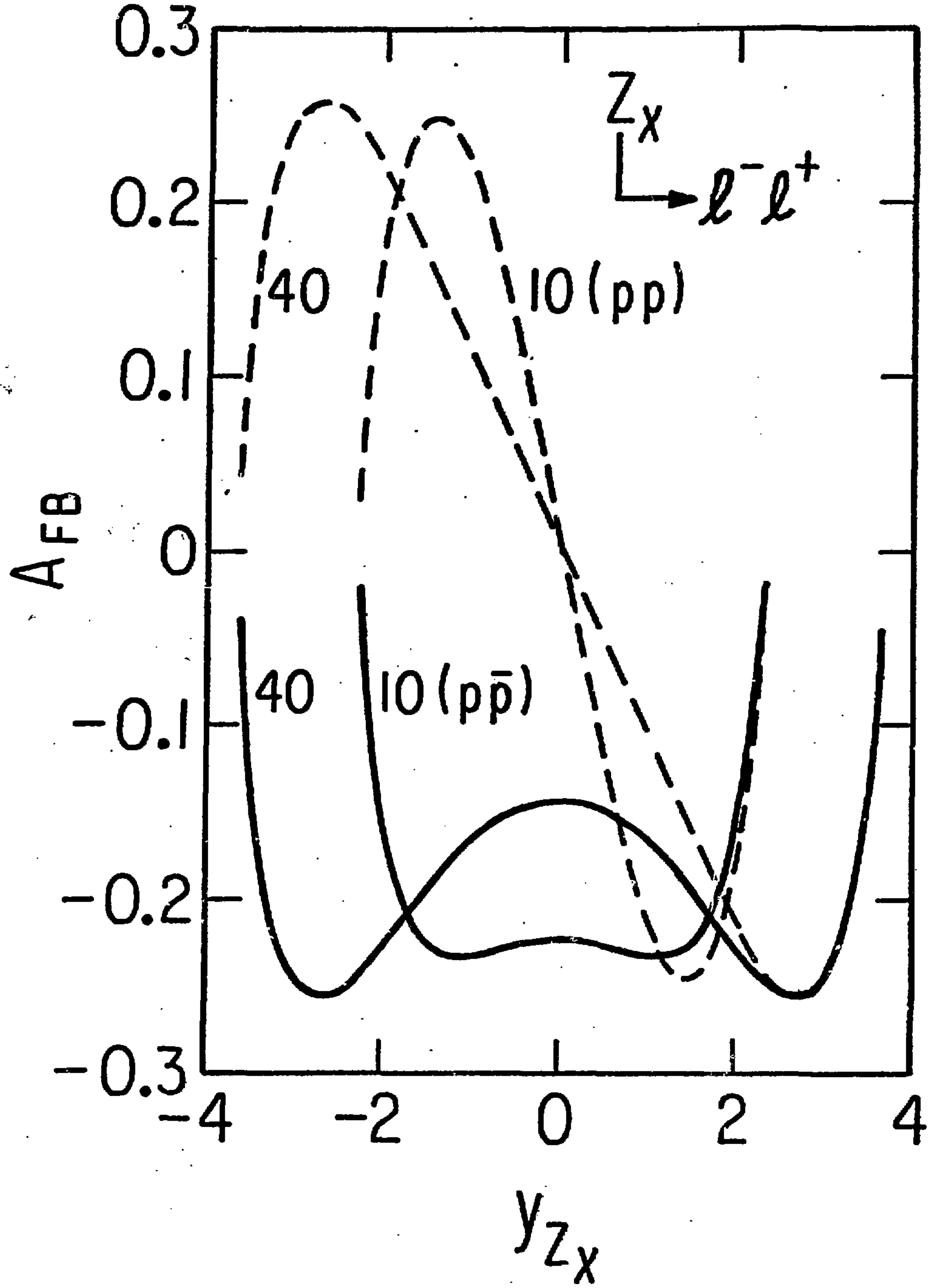

0.3
0.2
0.1
0
−0.1
−0.2
−0.3
A_{FB}
Z_χ
$\rightarrow \ell^- \ell^+$
40
10 (pp)
40
10 ($p\bar{p}$)
−4
−2
0
2
4
y_{Z_χ}

FIGURE 8